



Kochi Chapter

Indian Geotechnical Conference

IGC 2022

15<sup>th</sup> – 17<sup>th</sup> December, 2022, Kochi

## Liquefaction Analysis of Soil Profile Underneath the Multi Storey Building

Nimmy Ansly<sup>1</sup> Dr. K Ranga Swamy<sup>2</sup>

<sup>1</sup> Post Graduate Student, [nimmyansly257@gmail.com](mailto:nimmyansly257@gmail.com)

<sup>2</sup> Associate Professor, Department of Civil Engineering, NIT Calicut, Calicut -673601  
[ranga@nitc.ac.in](mailto:ranga@nitc.ac.in)

**Abstract.** Soil liquefaction occurs due to the loss of shear strength of saturated cohesionless soil under the influence of vibrations caused by seismic or dynamic events. Soil liquefaction can cause lateral spreading, ground settlement and sand boiling. Therefore, it is necessary to evaluate the safety of the ground supporting structures against soil liquefaction-induced ground damages. The present study focuses on liquefaction analysis of the soil profile underneath the multi-storey building structure due to the rise of pore pressure towards the foundation base. Modelling a multi-storey building is done using MIDAS GEN software. The analysis was conducted using the software MIDAS GTS NX and the nonlinear effective stress material model UBCSAND. The soil profile beneath the structure has been chosen with different soil layers, and the bottom of the soil profile is subjected to different PGA of seismic motion amplitudes. This study compares the liquefaction behaviour of a particular soil profile with and without a building structure subjected to seismic loading and also studies the behaviour of soil profile with the multi-storey building by varying the seismic and soil parameters. The results show that PGA, density and depth of liquefiable sand layer influence the liquefaction behaviour of the soil profile.

**Keywords:** Soil liquefaction, Seismic liquefaction analyses, MIDAS GTS NX, UBCSAND model.

### Introduction

#### Soil Liquefaction

Soil liquefaction is a significant geohazard triggered by seismic or dynamic events that gained the attention of the geotechnical engineering profession after the 1964 Niigata, Japan and Alaska, USA earthquakes. Liquefaction occurs in saturated, loose cohesionless soil under undrained conditions subjected to sudden shaking. During such an event, a rapid increase in pore pressures will trigger a significant decrease in effective stress, causing the soil to behave like a liquid. Loose saturated soil in undrained conditions

tries to rearrange the particles into a denser configuration, resulting in excess pore pressure build-up and thus susceptible to liquefaction. Liquefaction can affect the stresses acting on the soil and cause a consequent degradation of the soil's shear stiffness and strength, facilitating lateral spreading, ground settlement and sand boiling. The evidence of liquefaction-induced seismic settlements has been observed during past earthquakes such as the 1995 Hyogoken-Nambu earthquake, the 1999 Kocaeli earthquake, 1989 Loma Prieta in California and 2011 Christchurch in New Zealand.

The liquefaction phenomenon received lots of attention from the Geotechnical Engineering community. Many efforts have been made to study the primary mechanism and various aspects associated with liquefaction. Detailed investigation of liquefaction and its consequences have been studied by fewer researchers, including Yoshimi et al. (1977), Seed et al. (1979) and Finn. (1981). Liquefaction poses a severe risk of damage to the ground and the built environment. Settlement and lateral sliding occur due to liquefaction can damage the building foundation. Through centrifuge tests, Liu and Dobry (1997) initially developed correlations between the soil response and liquefaction-induced settlements. It proves that the foundation settled linearly with time during such events. The excess pore pressure below the foundation was below the pre-seismic level, while soil at the free field got fully liquefied.

Therefore, it is recognized that the structure's inertial forces influenced the building settlement. Dashti et al. (2010) conducted a series of centrifuge experiments to understand the mechanisms of seismic settlement during liquefaction. It studied the structure response on mat foundation on a layered liquefiable layer under various earthquake motions. Test results indicate the importance of the thickness and density of the liquefiable soil layer and the effects of different building and foundation characteristics on building performance. It compares the free-field soil response to that observed in the ground surrounding the structures. The experiments illustrated the complex interactions between key parameters, soil softening, and settlement mechanisms. A parametric study of seismic behaviour of soil-pile-structure interaction in liquefiable soils was conducted by B. K. Maheshwari and Rajib Sarkar (2011). It investigated the effect of loading intensity, soil stiffness, soil nonlinearity and pore pressure generation in the soil medium on the seismic behaviour of a pile group with structure. Karamitros et al. (2013) study focused on the excess pore-pressure build-up under the foundation, the seismic settlement accumulation, the static-bearing capacity degradation, and the inertia-induced interaction with the superstructure. It also found that the presence in the liquefiable soil prevents excess pore pressure ratios under the foundation from reaching the high free-field values.

Over the last few decades, estimation of liquefaction-induced damage continues to be based mainly on empirical equations. Many researchers have developed numerical simulations that helped predict the foundation's liquefaction behaviour when an earthquake strikes. To study the behaviour of sand during liquefaction, researchers have developed many constitutive sand models, including FINN, UBCSAND, UBC3D-PLM, HYPOPLASTICITY, HYPERBOLIC and BOUNDING SURFACE models etc. Numerical simulation of caisson type quay wall in the Kobe region of Japan, during which the Hyogoken-Nambu Earthquake shook in 1995, is done to judge the ability of the UBC3D-PLM constitutive model in simulating complex liquefaction behaviour (Galavi V. et al. (2013)). Daftari A. and W. Kudla (2014) compared the results of the UBC3D-PLM model with field data. Results showed similar trends between the UBC3D-PLM

model and reality. Many researchers have recently used PDMY02, PM4Sand and FINN soil models to predict the soil's liquefaction behaviour. Bray D. (2018) and Zana Karimi et al. (2018) did a parametric analysis to study the critical parameters affecting shear-induced liquefaction building settlement. It found that the key parameters influencing settlements are the density, depth, and thickness of the liquefiable layer, a thin low-permeability silty cap, and the spatial distribution of multiple layers. Foundation length-to-width ratio, bearing pressure, contact area, and embedment depth are essential factors affecting the behaviour.

Despite these well-documented past case histories, the relationship between critical parameters like soil properties, ground motion characteristics and foundation behaviour during liquefaction is not well understood. The present study focuses on liquefaction analysis of the soil profile underneath the multi-storey building structure due to the rise of pore pressure towards the foundation base. Modelling a multi-storey building is done using MIDAS GEN software. The analysis was conducted using MIDAS GTS NX software and the nonlinear effective stress material model UBCSAND used to model the liquefiable sand. The soil profile beneath the structure has been chosen with different soil layers, and the bottom of the soil profile is subjected to different PGA of seismic motion amplitudes. This study compares the liquefaction behaviour of a particular soil profile with and without a building structure subjected to seismic loading and also studies the behaviour of soil profile with the multi-storey building by varying the seismic and soil parameters.

## **Numerical modelling and analysis**

The present study analyses the liquefaction of the superstructure piled raft substructure foundation system under dynamic loading. Modelling the superstructure with 35 m height was done using structural software called MIDAS GEN software and exported to MIDAS GT NX software. The superstructure supported by the piled raft foundation embedded into the layered soil is modelled by MIDAS GT 3D finite element software. A licensed version of MIDAS GT NX 2017 (Version 1.1) is used for the present study. A space frame of a two-bay piled raft system with ten stories of the superstructure, having identical piles (25 nos.) spaced at 2.5m (2.5D), is used for the analysis. The pile length is 10m long and 1m in diameter. It uses a square raft of 15x15m and columns of 3.5m in length and 0.6m in width. The beams, columns, rafts and piles were made of concrete of grade M<sub>30</sub> is used in the analysis. The analysis is performed in stages of creating geometry, a constitutive model to predict the stress-strain response, mesh generation, structure and interface elements, loads and boundary conditions, and analysis control tools. The present model is validated by the data given on the model of quay wall supported on different soil layers subjected to seismic loading and coincides well with the results published by Galavi et al. 2013.

### **2.1 Material models and input parameters**

Different constitutive models and structural elements used to model the materials in the soil-piled raft-superstructure interaction modelling is shown in Table 1. Material properties are assigned to each material after the creation of the geometry of the model. The modified UBC sand model required additional input parameters for Layer 2 to simulate

the liquefaction susceptibility and corresponds to loosen sand with  $(N_1)_{60} = 10$  as presented in Table 2. The other parameters used are friction angle at constant volume ( $\phi_{cv}'$ ), elastic shear modulus number (keG), plastic shear modulus number (kpG), power for stress dependency of elastic and plastic shear modulus  $n_k$ ,  $n_g$ , and  $n_p$ ), failure ratio ( $R_f$ ), reference stress ( $P_A$ ), fitting parameter to adjust post liquefaction behaviour ( $fac_{post}$ ), and corrected SPT blow count. It referred to the published paper by Galavi V et al. (2013) to choose the different soil layers and assign the properties that depend on the state of the soil (loose, medium, and dense) and rock at the base of the soil profile.

**Table 1.** Input material parameters for the present constitutive models used.

Structural elements & Materials used	Structural elements and material models used	Input soil parameters					
		E (kN/m <sup>2</sup> )	$\nu$	$\gamma_b$ (kN/m <sup>3</sup> )	$\gamma_{sat}$ (kN/m <sup>3</sup> )	c, kPa	$\phi^\circ$
Beam & columns	Beam element	27390					
Slab beams	Plate element						
Raft	Plate element (elastic with $\mu=0.18$ )						
Pile	Beam element ( $\mu=0.18$ )						
Layered soil (thickness)							
Layer 1(5m)	Mohr Coulomb	30000	0.3	18	19	0	33
Layer 2(3m)	UBC sand (liquefiable)	24000	0.5	17	18	1	34
Layer 3(3m)	Mohr Coulomb	50000	0.2	19	21	0	36
Layer 4(5m)	Mohr Coulomb (rock)	360000	0.15	24	25	35	32

**Table 2.** Additional input material parameters for the Modified UBCSAND Model.

$\phi_{cv}'$	$k_e B$	$k_e G$	$K_p G$	$n_k$	$n_g$	$n_p$	$R_f$	$P_A$	$fac_{dens}$	$fac_{post}$
33	654	934	380	0.5	0.5	0.4	0.78	100	0.45	0.02

The soil continuum was modelled as different layers having different soil properties. The Mohr-Coulomb model was used to model medium sand (Layer 1), dense sand (Layer 3) and weathered rock (Layer 4). However, loose sand (Layer 2) was modelled with the UBC SAND constitutive model to assess the liquefaction susceptibility. The elastic model represents the raft, and the piles are modelled as a beam with an elastic model. The values of soil input parameters used for modelling are presented in Table 1. Layer 1 is medium-dense sand, and Layer 2 is loose sand. Therefore, the medium-dense sand layer (Layer 1) has a higher value of young's modulus. Poisson's ratio of 0.5 indicates the undrained state of the soil. The constitutive model requires the input of the saturated density of soil below the water table and bulk density to consider the

density of sand above the water table. Generally, fully saturated sand below the water table is susceptible to liquefaction due to the buildup of pore pressures.

## **2.2 Meshing and boundary conditions**

Mesh is generated on the created geometry model. It considers a very fine closer mesh in the vicinity of the structural elements. For all 3D structural elements, a hybrid mesh is used. A hybrid mesh with a mesh size of 0.5 is used for the raft. However, a mesh size of 1.2 had generated for the soil layer. Using GTS NX FE software, the degrees of freedom of a node are wholly or partially constrained.  $T_x$ ,  $T_y$ , and  $T_z$  are the displacement constraints in the x, y, and z directions and  $R_x$ ,  $R_y$ , and  $R_z$  are the rotational constraints in the x, y, and z directions. The bottom soil boundary is fully restrained from horizontal and vertical translations in this analysis. In the case of piles, the rotation in Z-axis is restricted.

Here, the numerical model considers each floor loaded with UDL of 3.5 kN/ m<sup>2</sup>. Therefore, total surcharge building load, including raft, pile and superstructure transfers to the foundation soil, is about 35 kN/m<sup>2</sup>. Eigenvalue analysis is used to analyze the inherent dynamic properties of the ground/structure, and this is used to obtain the natural mode (mode shape), natural period (natural frequency), modal participation factor etc. of the ground/structure. These properties are determined by the mass and stiffness of the system. The mass participation factor is a mass percentage factor representing how much of the structure participates in the vibration for each vibration mode when the structure is vibrated at a complex vibration mode. The earthquake wave's natural mode with a high mass participation factor is considered for analysis.

## **2.3 Liquefaction susceptibility of soil profile with and without building structure**

This paper compares the liquefaction response of soil profile in the free field and field with multistory building structures that act as additional surcharge weight. Nonlinear time history analysis was carried out to evaluate the liquefaction susceptibility of the particular soil profile with and without building structure subjected to earthquake time history. The 1968 Hokkaido earthquake, with a PGA of 0.132, is used as the seismic load time history for the analysis. One of the significant outcomes of nonlinear time history analysis is the pore pressure ratio generated during seismic load excitation. Based on pore pressure build-up criteria, soil liquefaction has defined as the state at which the excess pore water pressure ratio (PPR) equals 1.0. It occurs when the pore water pressure increase ( $\Delta u$ ) during seismic loading becomes equal to the initial vertical effective overburden stress ( $PPR = \Delta u / \sigma'_{v,0} = 1.0$ ) in the soil profile. The contours shown in Figs. 1 to 6 depict the pore pressure ratios of soil profile without and with building structure under seismic loading at different time intervals. It shows that the build-up of pore pressure in the soil profile is much higher than the soil profile with building structure subjected to seismic loading. It indicates that the soil profile without structure (free field) is highly susceptible to severe liquefaction than the soil profile with structure. The soil profile with the building structure resists the liquefaction may be due to an increase in overburden loads that leads to an increase in density, shear resistance and factor of safety against liquefaction. Hence, it proved that the soil profile with a multistory structure causes it to liquefy less compared with the free field soil profile. The reason is that the soil profile densifies with the overlying multi-storied

system, reducing pore pressure buildup. Building load is one of the parameters that affect the liquefaction of the soil profile nearby the foundation (R W Day, 2002).

Figs. 7 and 8 show the variation of PPR for soil profile with and without building structure subjected to seismic time history for 14 minutes duration. Even though the time taken to cause maximum pore pressure ratios is the same, about 4-5 seconds, the maximum pore pressure ratio developed in the soil profile is about 1.4 that higher than in the soil profile with structure. The maximum pore pressure ratios are stabilised after 4-5 seconds till continued up to 14 minutes. Even at initial time intervals of 2 and 3 seconds, the pore pressure build-up is higher in the soil profile than in the soil profile with the building structure. Pore pressure ratios developed in the soil profile without and with building structure has found to be about 0.78, 1.03 and 0.72, 0.91, respectively, at the time interval of 2 and 3 seconds. The soil profile in the free field is susceptible to initial liquefaction ( $\Delta_u / \sigma_{v,o} = 1.0$ ) at about 3 seconds; however soil profile with structure takes 5 minutes to initiate a state of liquefaction.

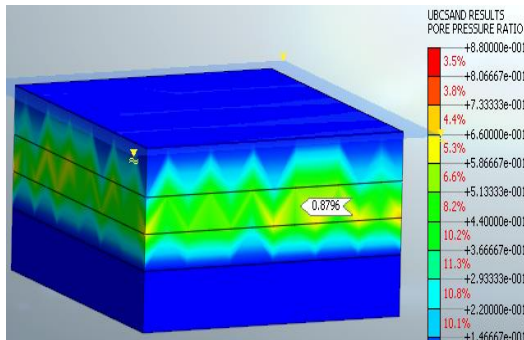


Fig. 1. PPR of soil profile (t = 2.4 sec.)

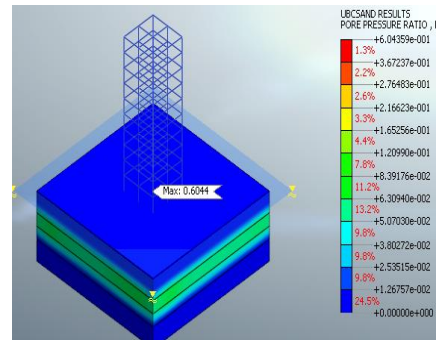


Fig. 2. PPR of soil profile with building structure (t = 2.4 sec.)

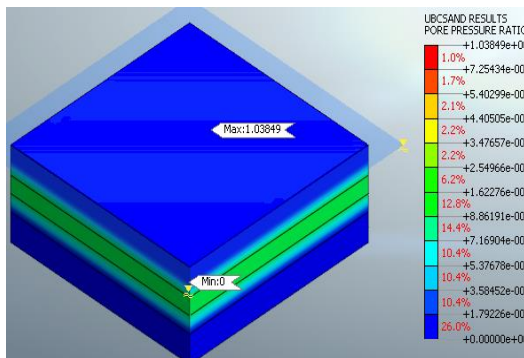


Fig. 3. PPR of soil profile (t = 2.8 sec.)

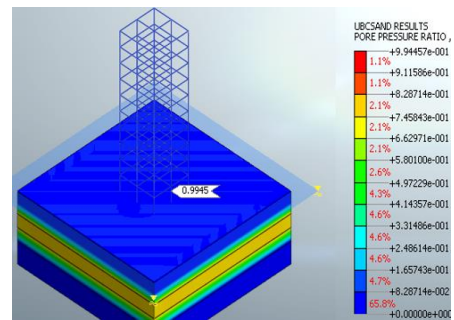


Fig. 4. PPR of soil profile with building structure (t = 2.8 sec.)

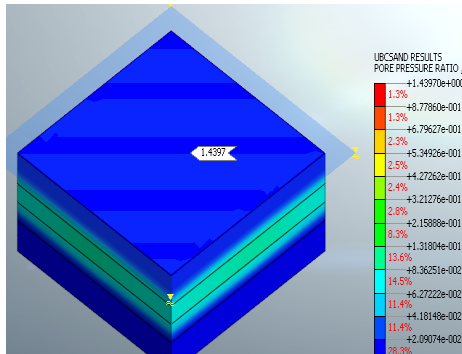


Fig. 5. Max. PPR of soil profile (t = 5 sec.)

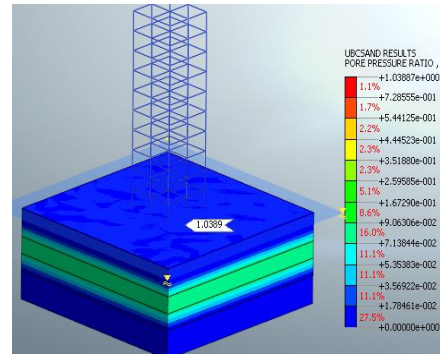


Fig. 6. Max. PPR of soil profile with building structure (t = 4 sec.)

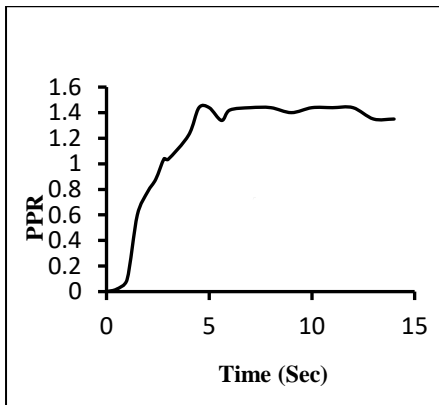


Fig. 7. Variation of PPR of soil profile

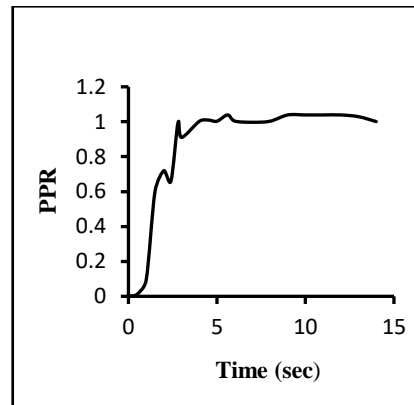


Fig. 8. Variation of PPR of soil profile with building structure

## 2.4 Peak ground acceleration

The present study is extended to study the effect of peak ground acceleration on the development of pore pressures and displacements of the soil profile with the building structure. Peak ground acceleration is a ground motion parameter of significant importance. The analysis is carried out for the PGA values of 0.104g, 0.155g, 0.214g and 0.275g. Based on the obtained contours from the FE analysis, the effect of PGA on the vertical and lateral displacement of the soil profile is shown in Fig. 9. Results reveal that the soil profile's deformations are influenced by the ground shaking at higher PGA values. The ground motion with a PGA of 0.1 shows the same amount of displacement of 6 cm in both the lateral and vertical directions of the soil profile. However, the lateral displacement is slightly higher than the vertical displacement of the soil profile with increased PGA of ground motion. The deformation of the soil profile with the building structure increases with the increase of PGA of ground motion. Fig. 10 shows a maximum pore pressure ratio developed in the soil profile subjected to seismic load with different PGA amplitudes. It had found that the build-up of pore pressures in the soil profile had increased with the amplitude of PGA of motion so that the soil profile is susceptible to liquefaction damages severely at higher PGA earthquake motions.

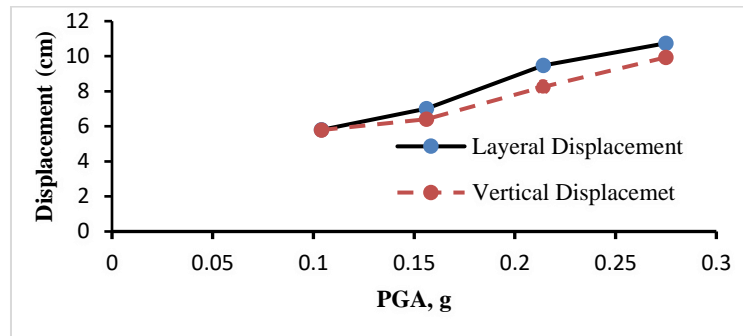


Fig. 9. Variation of displacement of soil profile with peak ground acceleration

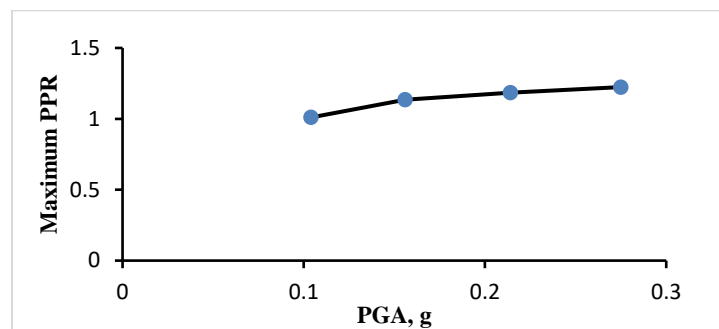


Fig. 10. Variation of maximum pore pressure ratio in soil profile with peak ground acceleration

### 2.5 Density of liquefiable sand layer

In the next phase, the numerical FE simulations were performed on the soil profile with structure after replacing the liquefiable sand layer of different densities. The density of the liquefiable sand layer changed from loose to dense ( $\gamma=16, 18, \text{ and } 20 \text{ kN/m}^3$ ) to study the effect of density on liquefaction susceptibility in terms of the maximum pore pressure ratio. Figs. 11 to 13 show the contours of development of pore pressure ratios in the soil profile with different densities of the liquefiable sand layer. From the contours, maximum pore pressure ratios are traced and plotted in the relationship between the density and maximum pore pressure ratio in the soil profile, as shown in Fig. 14. It is understood that the maximum pore pressure ratio decreases with the density of the liquefiable sand layer increases. Hence, the soil profile with a loose liquefiable sand layer causes severe liquefaction susceptibility. The dense sand layer is dilative, making it less susceptible to liquefaction.



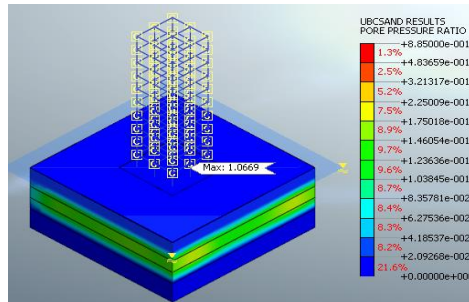


Fig. 11. PPR of soil profile ( $\gamma=16 \text{ kN/m}^3$ )

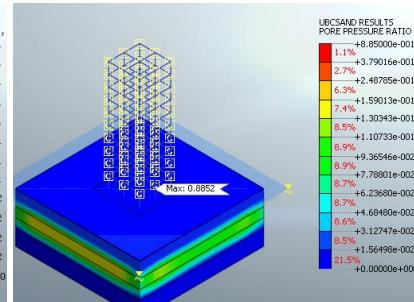


Fig. 12. PPR of soil profile ( $\gamma=18 \text{ kN/m}^3$ )

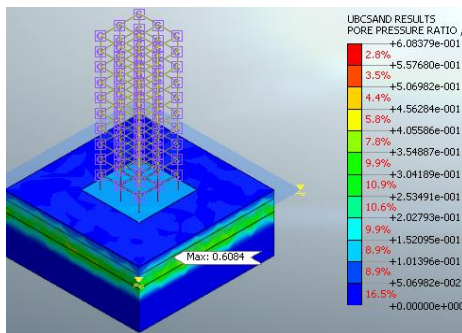


Fig. 13. PPR of soil profile ( $\gamma=20 \text{ kN/m}^3$ )

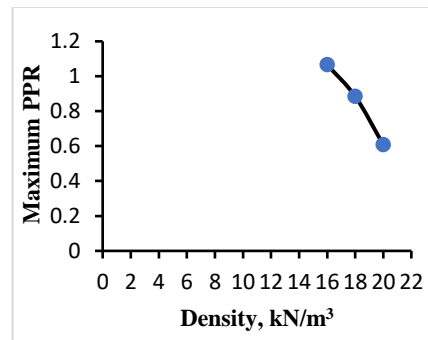


Fig. 14. Variation of maximum PPR with density of liquefiable sand

## 2.6 Depth of liquefiable sand layer

The present study also examines the effect of the depth of the liquefiable sand layer below the foundation substructure on the development of maximum pore pressures and progressive displacements in the soil profile subjected to seismic load. Fig. 15 shows the variation of maximum pore pressure ratios with a depth of liquefiable sand layer on soil profile subjected to the time history of the 1968 Hokkaido earthquake. The outcome seems to be the reduction in the maximum pore water pressure ratio with an increase in the depth of the liquefiable sand layer below the base of the foundation. The soil profile could not liquefy if the non-liquefiable surface layer (generally clay layer) thickness below the foundation increases from 2 to 11 m. It is well agreed with published literature. The soil profile and substructure cause severe liquefaction if the liquefiable sand layer exists at a shallow depth below the foundation base. Not only the reduction of pore pressures but also the settlements and deformations are reducing drastically with an increase in the depth of the liquefiable sand layer, as shown in Fig. 16.

Vertical settlement of soil profile is slightly less than lateral deformations irrespective of the depth of the liquefiable sand layer. Hence, it requires a sufficient increase in the depth of cohesive unliquefiable clay surface layer just below the foundation to prevent liquefaction susceptibility.

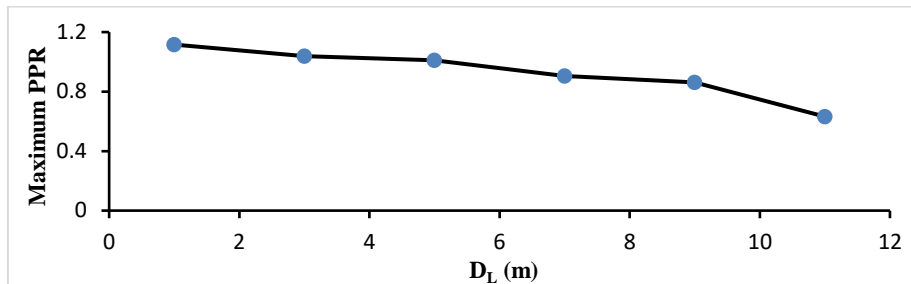


Fig. 15. Variation of maximum PPR with depth of liquefiable sand layer

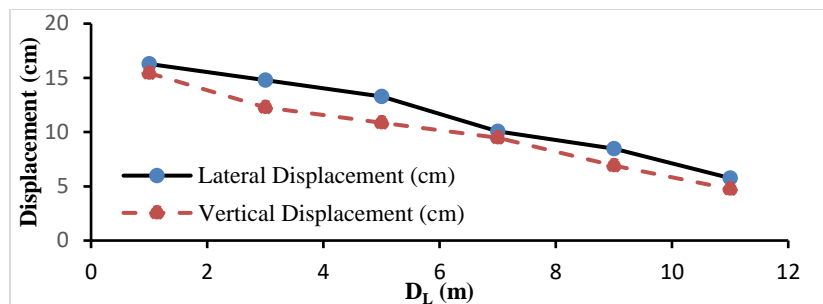


Fig. 16. Variation of displacement of soil profile with depth of liquefiable sand layer

## Conclusions

The present study focuses on the liquefaction susceptibility of soil profile underneath the multi-storey building structure. The seismic analysis of layered soil profile with a liquefiable sand layer using time history analysis is performed using the finite element software MIDAS GTS NX and the nonlinear effective stress material model UBCSAND. The significant conclusions arrived from the present study are:

- Excess pore pressure ratios developed in the soil profile beneath the foundation of a multi-storey building are substantially less than the soil profile in free field conditions because increased vertical stress induced by the building structure leads to densifying the ground.
- The build-up of pore pressures, settlement and displacements in the soil profile had increased with the amplitude of PGA of motion so that the soil profile is susceptible to liquefaction damages severely at higher PGA earthquake motions.
- The maximum pore pressure ratio decreases with the density of the liquefiable sand layer increases. Hence, the soil profile with a loose liquefiable sand layer causes severe liquefaction susceptibility.
- Not only the reduction of pore pressures but also the settlements and deformations are reducing drastically with an increase in the depth of the liquefiable sand layer.

## References

1. B. K. Maheshwari and Rajib Sarkar, 2011, Seismic Behaviour of Soil-Pile-Structure Interaction in Liquefiable Soils: Parametric Study, *International Journal of Geomechanics*, Vol. 11, No. 4.
2. Daftari A., and W. Kudla, 2014, Prediction of Soil Liquefaction by Using UBC3D-PLM Model in PLAXIS, *International Journal of Civil and Environmental Engineering* Vol:8, No:2, 2014.
3. Dimitrios K. Karamitros, George D. Bouckovalas and Yannis K. Chaloulos, 2013, Insight into the Seismic Liquefaction Performance of Shallow Foundations, *Journal of Geotechnical and Geoenvironmental Engineering* ©ASCE, ISSN 1090-0241.
4. Finn W. D. (1981). Liquefaction potential: Developments since 1976., *Proc. Of Ist Int. conference on recent advances in Geotechnical Earthquake Engineering and Soil Dynamics*, April 26 to May 3, 1981, St. Louis, Missouri. P: 655-681.
5. Jorge Macedo, and Jonathan D. Bray, 2018, Key Trends in Liquefaction-Induced Building Settlement, *Journal of Geotechnical and Geoenvironmental Engineering*, © ASCE, ISSN 1090-0241.
6. Lee Lin and Ricardo Dobry, 1997, Seismic response of shallow foundation on liquefiable sand, *Journal of Geotechnical and Geoenvironmental Engineering*, Vol. 123, No.6, June.
7. Shideh Dashti, Jonathan D. Bray, Juan M. Pestana, Michael Riemer and Dan Wilson, 2010, Mechanisms of Seismically Induced Settlement of Buildings with Shallow Foundations on Liquefiable Soil, *Journal of Geotechnical and Geoenvironmental Engineering*, Vol. 136, No. 1.
8. Shideh Dashti, Jonathan D. Bray, Juan M. Pestana and Michael Riemer, 2010, Centrifuge Testing to Evaluate and Mitigate Liquefaction-Induced Building Settlement Mechanisms, *Journal of Geotechnical and Geoenvironmental Engineering*, Vol. 136.
9. H. Bolton Seed, Soil Liquefaction and Cyclic Mobility Evaluation for Level Ground During Earthquakes, *Journal of the Geotechnical Engineering Division, ASCE*, Vol.105, No.GT2, Feb., pp.201-255 (1979).
10. R W Day, 2002. *Geotechnical Earthquake Engineering handbook*. SBN: 9780071377829. The McGraw-Hill Companies, Inc.
11. V. Galavi, A. Petalas and R.B.J. Brinkgreve, 2013, Finite Element Modelling of Seismic Liquefaction in Soils, *Geotechnical Engineering Journal of the SEAGS & AGSSEA* Vol. 44 ISSN 0046-5828
12. Yoshiaki Yoshimura and Kohji Tokimatsu (1977), settlement of buildings on saturated sand during earthquakes, *SOILS AND FOUNDATIONS* Vol. 17, No. 1.
13. Zana Karimi, Shideh Dashtia, Zach Bullocka, Keith Portera and Abbie Liel, 2018, Key predictors of structure settlement on liquefiable ground: a numerical parametric study, *Soil Dynamics and Earthquake Engineering* 113 (2018) 286–308.